Welding in the World (2020) 64:1175–1183
https://doi.org/10.1007/s40194-020-00910-6

RESEARCH PAPER

Influence of mill scale on weld bead geometry and thermal cycle during GTA welding of high-strength steels

Rahul Sharma[1] · Uwe Reisgen[1]

Received: 21 November 2019 / Accepted: 24 April 2020 / Published online: 5 May 2020

Abstract
High-strength steel heavy plates are usually covered with a mill scale after production. Morphology, structure, and chemical composition are determined by several factors, e.g., rolling parameters, cooling rate, quenching method, and alloying elements. As the mill scale might cause pore formation and process instability, it is preferably removed prior to welding. In welding practice, the removal of scale is in many cases insufficient and can lead to welding defects. In this paper, the influence of a scale layer on the weld bead geometry and thermal cycle during GTA welding is analyzed. Several high-strength steels with different chemical compositions and plate thicknesses have been used for bead-on-plate welding. The influence of mill scale on penetration depth and cooling time is analyzed and a connection to the varying fluid flow in the weld pool is drawn.

Keywords Cooling rate · GTA welding · Low-alloyed steel · Micro-alloyed steel · Temperature · Weld shape

1 Introduction

The application of high-strength steels in engineering construction and manufacturing of mechanical components is continuously increasing as these steels offer improved properties compared with carbon-manganese steels with lower tensile strength.

High-strength steels are mostly low-alloyed ferritic steels with additions of manganese, silicon, chromium, molybdenum, nickel, copper, and micro-alloying elements such as vanadium, niobium, titanium, aluminum, and zirconium. During cooling, they undergo a solid-state phase transformation from austenite to ferrite, resulting in a microstructure, which is composed in varying portions of ferrite, pearlite, bainite, and martensite.

To achieve high yield strength, notch impact toughness, and good weldability, the carbon content of these steel grades is restricted to low values. Further alloying elements are therefore added which lead to transformation retardation. Besides the quenched and tempered steel grades (QT) with the highest yield strength, thermomechanically controlled processed heavy plates (TMCP) are available on the market up to 960-MPa yield strength [1].

Heavy plates are usually covered with scale and rust layers, which are a result of hot rolling, cooling process, and storage under atmospheric conditions. The oxide content in the superficial layer leads to changed weld pool behavior as fluid flow and arc geometry are influenced by oxygen partial pressure [2, 3]. Therefore, the resulting weld bead geometry changes if scale layers are not completely removed.

During hot rolling of metals, a mill scale is formed on the strip surface as processing is usually carried out at atmospheric conditions. The scale layer consists of a mixture of the iron oxide phases: magnetite (Fe_3O_4), hematite (Fe_2O_3), and wustite (FeO) [4]. During cooling, the composition of the oxide scale changes, as hematite is preferably formed in regions with high oxygen partial pressure. Formation and growth of the scale layer are temperature and time dependent and start from the first heating of the heavy slabs in the furnace. The primary and secondary scale layer which form are partially removed by high-pressure water jets before the slab enters the finishing mill (Fig. 1). During and after hot rolling,

Recommended for publication by Commission IX - Behaviour of Metals Subjected to Welding

✉ Rahul Sharma
sharma@isf.rwth-aachen.de

Uwe Reisgen
head@isf.rwth-aachen.de

[1] Welding and Joining Institute, RWTH Aachen University, Aachen, Germany

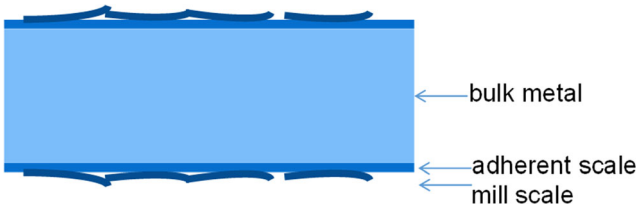

Fig. 1 Simplified structure model of scale layer on hot rolled steel plates

the tertiary scale grows until the temperature drops below 500 °C and remains on the surface. For the surface quality of the finished product, it is crucial to have a uniform oxide layer. Depending on its thickness and morphology, the scale layer must be removed prior to apply the following joining and surfacing processes. For the welding of steels, the scale layer is removed in most cases in order to follow international codes and guidelines for good welding practice [5]. One of the main reasons therefore lies in the undefined properties of the scale layer, which leads to varying weld pool geometry and arc characteristics. Furthermore, the brittle surface structure can form deposits of moisture and oil.

High-strength steel heavy plates with yield strength levels above 500 MPa are increasingly produced by thermomechanical treatment with controlled cooling as weldability improves with decreasing carbon content. Besides that, quenched and tempered production of heavy plates is still very important. The differing chemical composition and thermal cycle leads to a changed surface oxide layer with varying porosity and structure. The oxide growth kinetics, chemical composition, and the deformation temperature define the thickness and pore distribution in steels and lead to a scale layer morphology typical for the method of steel production [4, 6].

The weld pool fluid flow phenomena in gas tungsten arc welding are, besides other influencing factors, strongly guided by the chemical composition of the base material. The addition of surface-active elements, such as selenium and cerium are known to have a strong influence on the weld appearance [7]. For low sulfur steels, the quantity of oxygen and reductive additions becomes more important. This is the case for most modern high-strength steels, which contain only very low amounts of sulfur [8]. When a scale layer on the base metal surface is remelted by the GTA process, the oxygen partial pressure in the arc column, and therefore in the weld pool, rises. This leads to a changed weld pool fluid flow behavior and weld pool geometry. The main reason for this is seen in the changed surface tension gradient [8].

The influence of a remelted mill scale on the weld bead geometry has been observed in [2, 15]. Two high-strength steel grades of differing chemical composition and delivery state led to differing weld bead geometry during GTA remelting with or without mill scale. The authors assume surface tension gradient changes are responsible for the observed behavior. However, the surface conditions and the oxygen concentrations in the weld metal are not given.

Based on the aforementioned remarks, an experimental investigation was designed to show the fundamental effect of oxide scale layers melted by a welding arc. Therefore, the GTA welding process was chosen in order to separate alloying effects of the welding filler metal.

Table 1 Base metal sample plate thickness

S690QL	S700MC	S960QL	S960MC	S1100QL
10 mm	12 mm	12 mm	12 mm	11 mm

2 Experimental approach

In the present study, five different high-strength steel types were compared after GTA welding of a single-bead-on-plate weld run. For the first part of the welding experiment, the sample coupons were cut from heavy plates in delivery condition (covered with scale). For every steel type, four bead-on-plate weld runs were carried out with differing heat input on sample plates of the area 220 mm × 100 mm. The sample thickness is given in Table 1. The purpose of this experiment was to investigate if any relationship between varying weld bead geometry and heat input could be observed when remelting the sample plates covered with mill scale. Since the base plates had a slightly varying thickness and surface roughness, in a second step, another set of plates was machined to a total thickness of 10 mm from the backside. It was intended to achieve equal heat dissipation conditions during the experiments through this measure. For these welds, only welding parameter set A was used (Table 3).

The chemical composition of the steel plates investigated is typical of high-strength steels at the upper strength level (Table 2). It was determined using spark optical emission spectrometry. The sulfur content was measured by

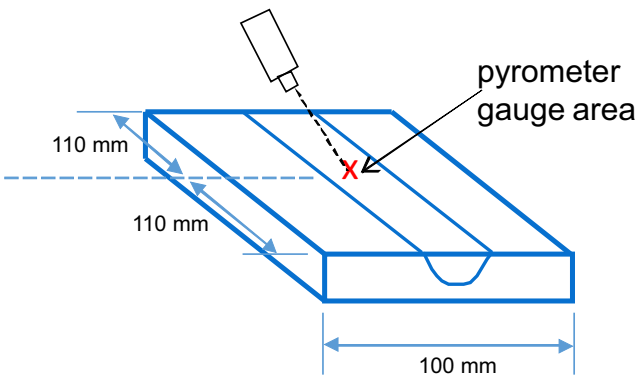

Fig. 2 Schematic sample plate with a marked area of temperature measurement

Table 2 Chemical composition of base metal, determined using spark OES, Fe = balance

Weight (%)	C	Si	Mn	P	S*	Cr	Mo	Ni	Al	Nb	V	Ti	B	Se	Ce	O*
S690QL	0.14	0.27	1.2	0.019	10	0.33	0.21	0.04	0.082	0.030	0.007	0.003	0.0015	0.004	0.006	24
S700MC	0.04	0.35	1.9	0.008	12	0.16	0.12	0.15	0.030	0.041	0.009	0.014	0.0008	0.007	0.007	39
S960QL	0.11	0.26	1.1	0.013	15	0.60	0.31	0.37	0.076	0.028	0.055	0.005	0.0010	0.005	0.007	13
S960MC	0.08	0.34	1.7	0.010	10	0.60	0.29	0.03	0.034	0.034	0.079	0.014	0.0009	0.006	0.007	27
S1100QL	0.12	0.23	0.9	0.008	11	0.61	0.61	1.84	0.035	0.022	0.005	0.003	0.0006	0.005	0.006	13

*ppm, determined using a combustion analysis

combustion analysis. Besides carbon, manganese, and silicon, the alloying concept is based on chromium, molybdenum, and micro-alloying elements. For S960QL and S1100QL, significant amounts of nickel can be found, which is typical for these steels. The sulfur content in all samples was found to be between 10 and 15 ppm, which is typical for current high-strength steels of yield strength levels higher than 690 MPa. Other surface-active elements (Se, Ce) were only found in low concentrations.

For the welding experiments, the surface of all sample plates was cleaned using acetone to remove all organic residues. Every experiment was then carried out on a sample plate with a mill scale left on the surface and repeated on a sample plate where the mill scale was removed beforehand with a disk grinding machine.

The welding setup consisted of a GTA welding power source with water-cooled welding torch and a movable sample table. Above the sample, a pyrometer was mounted to measure the transient temperature curve in the weld metal during cooling in the center of the weld bead (Fig. 2). The measurement position was kept constant during all experiments. The calibration procedure used is described in ref. [9]. The idea of measuring the cooling time in all experiments was to separate effects of varying thermal conditions and weld pool phenomena. All trials were carried out using argon shielding gas ISO 14175-I1 (4.6), electrode-to-workpiece-distance of 2 mm, a gas nozzle width of 15 mm, and mixed rare earth oxide doted electrode (unthoriated, EN ISO 6848 WG) of 3.2-mm diameter.

In order to analyze the influence of mill scale on the cooling times on the weld bead geometry, four welding parameter sets were specified (Table 3). The arc energy was changed in every set by adjusting the welding speed. Even if the arc energies considered are typical for automatic welding of high-strength steels up to 1100-MPa yield strength, it has to be noted that the working window for such steels usually is between 6 and 15 s [10] in practical applications to ensure good mechanical properties. In order to get a rough estimate of the resulting cooling times, values calculated based on the arc energy are given (Table 3). A preheating temperature of 100 °C was used throughout the experiments. In order to reduce the level of moisture and residual organic compounds, the preheating temperature was held for 30 min prior to welding. In a preliminary experiment, the diffusible hydrogen concentration in mill scale-covered samples of the base materials was determined using the procedure described in ISO 3690 (TGS, sample geometry C, measurement temperature 400 °C, duration 30 min.). The measurement was performed after heating the samples to 100 °C over a period of 30 min. No higher diffusible hydrogen concentration than 0.1 ppm was found within the investigated steels.

After performing the weld runs on the sample plates, macro cross sections were prepared in order to analyze the weld bead geometry. Chemical analyses of the weld metal were performed by using the same methods applied on the base metal. Within cross sections of mill scale-covered samples, SEM analyses of the surface zone were carried out to investigate

Table 3 GTA welding parameter sets

	Arc energy (kJ/cm)	Voltage (V)	Current (A)	Welding speed (cm/min)	Calc. cooling time $t_{8/5}$* (s)
A	16	14	200	10.5	11.3
B	11.6			14.6	8.2
C	7			24	5.0
D	5			33.6	3.5

*Calculation based on the formula given in DIN EN ISO 1011-2 for 12-mm plate thickness, 3D heat dissipation, thermal efficiency $\eta = 0.6$

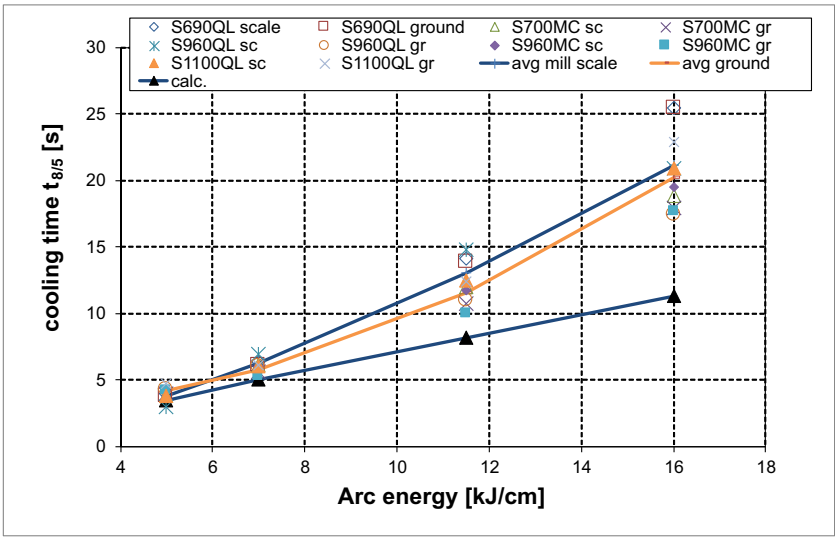

Fig. 3 Cooling times $t_{8/5}$ for specific arc energy with average curves of mill scale-covered and ground surface samples and calculated cooling times $t_{8/5}$ acc. to Table 3

the thickness, morphology, and chemical composition of the mill scale layer.

3 Results

The measured cooling times from 800 to 500 °C for varying arc energies are given in Fig. 3. The average curves for the cooling times of samples with mill scale left and mill scale removed prior to welding shows that oxide layers on the surface lead to slightly higher cooling times. It is obvious that the measured cooling times are higher than the calculated ones. Taking these observations into account, it was decided to repeat one parameter set with an adapted uniform sample thickness of 10 mm. This was achieved through one-sided machining of all samples. The parameter set of 16 kJ/cm was chosen in order to improve the detectability of any possible weld pool geometry change.

It can be seen that weld runs on mill scale-free sample plates lead to shorter cooling times (Fig. 4). Furthermore, the cooling time varies between different steel grades. Compared with the aforementioned results (Fig. 3), it has to be considered that the flat backside and the uniform surface condition enables heat conduction into the sample holder (a flat steel plate), which seems to be the main reason for much shorter cooling times achieved here.

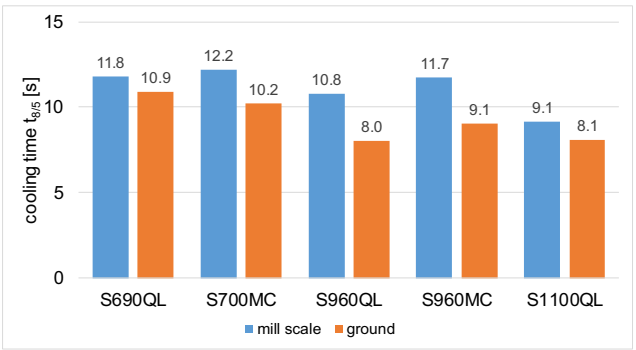

Fig. 4 Cooling times $t_{8/5}$ for uniform plate thickness of 10 mm, welding parameter set A, arc energy 16 kJ/cm

When looking at the weld bead geometry, it is notable that the mill scale left on the surface leads to decreased weld width in most cases. At the same time, the penetration depth increases drastically (Fig. 5), resulting in a depth-to-width ratio between 0.5 and 0.6 (Fig. 6) except for S690QL where the penetration depth is reduced in case of the scale-covered sample. The consideration of the total cross-sectional weld bead area shows that the mill scale leads to an increased weld bead area, which is in correspondence with the increased cooling times (Fig. 7 and 8).

The chemical analysis of the weld metal showed that during GTA remelting only very small amounts of chemical composition changes occurred (Table 4), compared with the base metal (Table 2), which is typical for the GTA welding process. A slight burn off of reactive elements (C, Mn, Al, Ti) was found. At the same time, the oxygen content on the other hand increases considerably for the remelted scale-covered samples (Fig. 9).

Since weld metal oxygen content tends to affect the mechanical properties of low-alloyed steel weld metals, hardness measurements were carried out. Average values of five hardness indentations within the weld metal are given in Fig. 10. For the steel S1100QL, no difference in hardness could be found when the mill scale was left on the surface. All other samples show slightly higher hardness values for the ground surface. A notable increase of 50 HV1 could be observed within the S960QL sample.

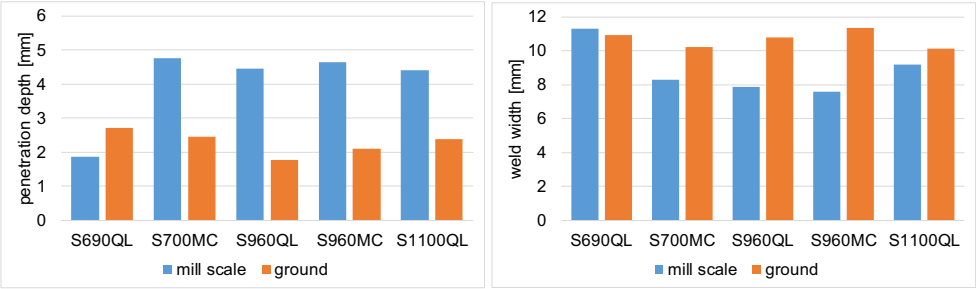

Fig. 5 Comparison of weld penetration (left) and width (right) for GTA welds in scale-covered and ground condition, welding parameter set A, arc energy 16 kJ/cm

A closer analysis of the scale layer was done through a scanning electron microscope (SEM) imaging and energy dispersive X-Ray analysis (EDX) in cross sections of the scale layer (Fig. 8 and Table 5). The scale layer morphology of QT steels differs from the scale layer of TMCP steels. For the QT steels, the mill scale showed a porous and irregular structure, whereas the TMCP steels formed very uniform and dense oxide scales. The porosity of the scale increased with a higher nickel content of the steel, which is in agreement with information reported in [11].

For the determination of the chemical composition of the mill scale, EDX measurements were performed during SEM analysis of scale layer cross sections (Table 5). The main constituents of the scale layers besides oxygen and iron are manganese and chromium. It was found that no significant difference between the steel grades existed, taking into account that the detection limit of EDX analysis is not suitable for trace elements. Furthermore, the analysis was carried out as a point analysis, which is the only representative of specific scale microstructure constituents. This is also the reason for the high contents of chromium and molybdenum found in S1100QL.

For all steel grades, the average thickness of the mill scale layer was between 9 and 17 μm (Table 6). The lowest average thickness was found on the S690QL steel. It can be seen that the samples with lower scale layer thickness also contain less oxygen in the weld metal, when the scale layer is remelted (Fig. 9).

4 Discussion

The remelting of mill scale-covered steel leads to increased cooling times, which corresponds mostly to the changed weld pool geometry. As the electrical parameters of the arc and the arc energy did not change by more than ± 2%, the different weld bead geometry must be caused by changes in heat conduction conditions. This happens when the fluid flow inside the weld pool is changed. As a result, the penetration depth varies within the order of magnitude of the plate thickness. Since the thickness of the sample plates was relatively thin, the heat dissipation from the weld zone is influenced by the distance from the fusion line to the backside of the plate. The backside of the sample plate leads to heat accumulation due to the lower heat transfer at the surface compared with the bulk material. For deeper penetration welds, the state of planar heat conduction parallel to the plate plane is achieved faster. This corresponds to the appearance of the HAZ in the macro sections (Fig. 8). The only steel grade that showed nearly no change in weld bead geometry with mill scale was the S690QL.

Higher alloying element concentrations seem to lead to shorter cooling times, since the solid-state phase transformation temperature decreases with a higher content of diffusion slowing elements so that the release of latent heat does not contribute to the cooling time $t_{8/5}$ in some cases. This happens when the transformation temperature lies outside of the considered temperature range, as it has been already reported in refs. [9, 11].

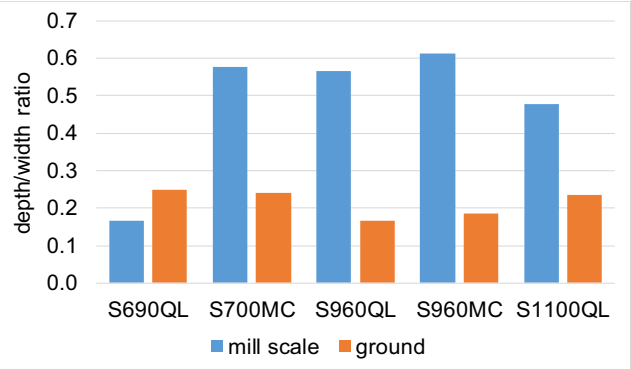

Fig. 6 Penetration depth/width ratio of the welds, parameter set A, arc energy 16 kJ/cm

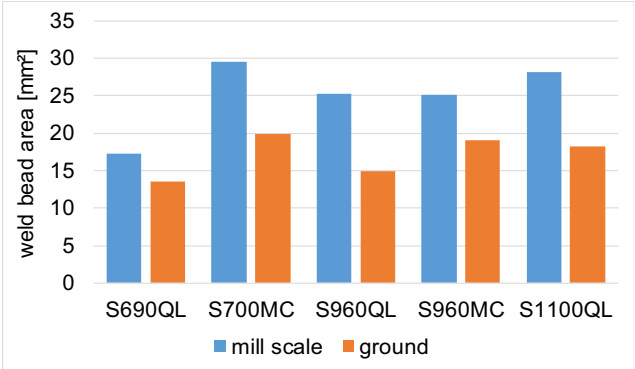

Fig. 7 Total weld bead cross-sectional area, parameter set A, arc energy 16 kJ/cm

Table 4 Chemical composition of all welds with 16 kJ/cm

Weight (%)		C	Si	Mn	P	S*	Cr	Mo	Ni	Al	Nb	Ti	Se	Ce
S690QL	Mill scale	0.14	0.27	1.17	0.019	18	0.34	0.21	0.04	0.060	0.029	0.002	0.005	0.006
	Ground	0.15	0.26	1.16	0.018	25	0.33	0.21	0.04	0.077	0.029	0.003	0.004	0.005
S700M*	Mill scale	0.03	0.31	1.85	0.018	18	0.15	0.10	0.12	0.020	0.032	0.009	0.008	0.005
	Ground	0.04	0.32	1.81	0.015	12	0.15	0.10	0.12	0.026	0.032	0.011	0.006	0.004
S960QL	Mill scale	0.14	0.26	1.14	0.014	10	0.61	0.32	0.36	0.042	0.028	0.005	0.005	0.007
	Ground	0.13	0.26	1.15	0.014	8	0.61	0.32	0.37	0.068	0.029	0.005	0.005	0.006
S960M	Mill scale	0.07	0.32	1.62	0.009	11	0.60	0.29	0.03	0.023	0.034	0.011	0.005	0.006
	Ground	0.07	0.34	1.67	0.010	8	0.60	0.29	0.03	0.032	0.035	0.014	0.007	0.006
S1100QL	Mill scale	0.16	0.20	0.86	0.009	14	0.61	0.61	1.94	0.022	0.023	0.002	0.007	0.007
	Ground	0.13	0.23	0.93	0.008	15	0.61	0.61	1.85	0.030	0.022	0.003	0.004	0.006

*ppm

The small burn off of reactive elements is a possible indication for higher oxygen potential in the weld pool, when the scale layer is remelted. This can be verified by the higher oxygen concentrations found in the weld metal (Fig. 9) in comparison with the base metal. As surface-active elements were found only in small concentrations in all weld metals, it is suggested that the change in oxygen potential when remelting the mill scale is the most important influencing

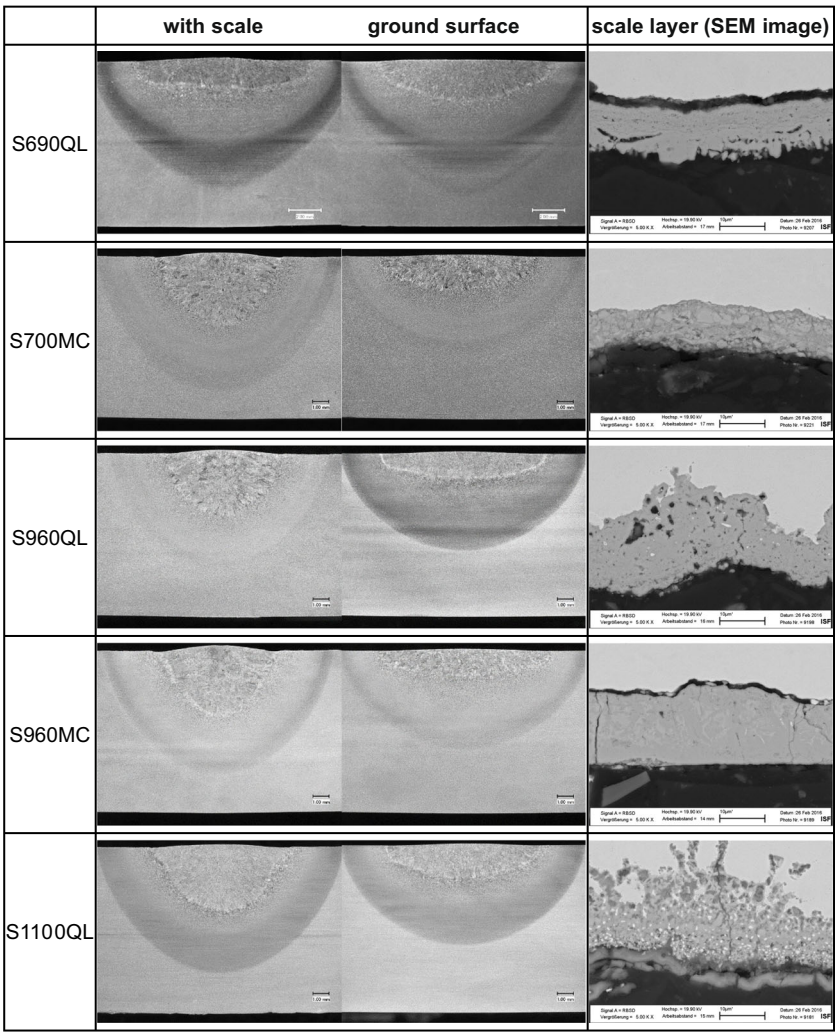

Fig. 8 Cross sections of all welds with 16 kJ/cm and SEM images of the scale layer structure

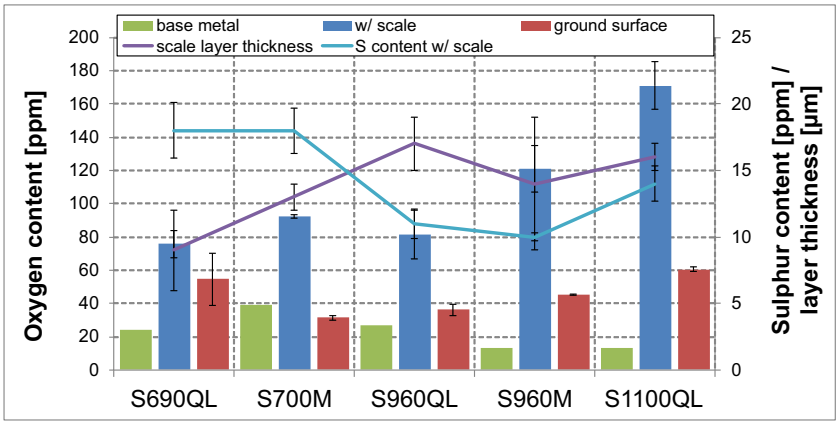

Fig. 9 Comparison of oxygen content, sulfur content, and scale layer thickness

factor on the weld bead geometry. Due to the very low sulfur content, oxygen has a stronger influence on the surface tension gradient and therefore leads to increased penetration depth [8]. This could be one possible explanation of why the strong increase in penetration depth was not observed in the past. The amount of slag islands on the solidified weld bead was even low at the oxide scale-covered samples (Figs. 11 and 12). Nevertheless, a change in fluid flow can be also induced through any change in arc-plasma interaction, which is to be investigated in future experiments. While the behavior of most of the investigated materials can be explained by this, it remains open why only a small change in penetration depth can be found when welding the S690QL. Considering the lower scale layer thickness, the low oxygen concentration, and the slightly higher content of sulfur, carbon, and aluminum, it is presumed that these influencing factors cause only a slight change in weld pool fluid flow in this steel grade. Moreover, the methods applied to determine the oxygen content are unable to determine the oxygen activity in the weld pool. This depends on the amount of other reactive elements within the liquid metal.

The change in hardness of the samples can be explained when considering the cooling time difference in Fig. 5. A clear correlation between hardness and cooling time was observed. On the other hand, the increased oxygen content did not seem to influence the hardness of the samples (Fig. 10). For S1100QL, the oxygen content shows a strong increase, while, at the same time, no change in hardness was observed. As S1100QL forms a microstructure with higher martensite content compared with the other investigated steels, it is comprehensible that the cooling time is more dominant than the availability of nucleation sites for ferritic or bainitic transformation. The low hardness level of remelted S960M becomes understandable when the chemical composition is taken into account. The strength level of 960-MPa yield strength is based on the thermomechanical processing of this steel but does not appear within a remelted weld metal of this composition.

It is expected that the oxygen content influences the toughness level of the weld metal since the formation of inclusions is guided by the oxygen potential in the weld zone [12]. The resulting oxygen levels are still below values typical for other arc welding methods [13].

The morphology and chemical composition did not seem to have any specific influence on the increase of penetration depth. Mostly the increased oxygen potential led to a changed weld pool behavior. Higher layer thicknesses led to the higher oxygen content in the weld metal and higher penetration depths. However, the scale layer thickness is essentially determined by the rolling parameters and product thickness.

Generally, the investigation presented here could not clearly establish a single mechanism which is responsible for the observed change in weld bead geometry. Although the oxide concentration seems to play a significant role, quantitative

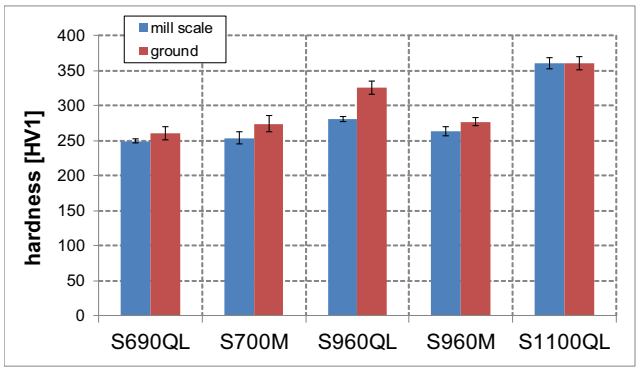

Fig. 10 Average weld metal hardness ($n = 5$)

Table 5 Chemical composition of base metal scale layer (EDX analysis)

Weight (%)	O	Si	Cr	Mn	Fe	Ni	Mo
S690QL	20	0.1	0.3	0.7	79	-	0.0
S700MC	15	0.1	0.4	1.7	83	-	0.1
S960QL	17	0.3	1.0	1.3	80	-	0.1
S960MC	17	0.2	0.5	1.2	81	-	0.1
S1100QL	21	0.5	2.2	0.5	70	1.9	3.4

Table 6 Scale layer thickness (cross-section SEM image measurement)

	Layer thickness (μm)
S690QL	9 ± 3
S700MC	13 ± 1
S960QL	14 ± 2
S960MC	17 ± 5
S1100QL	16 ± 1

consideration of the influencing factors would be appreciable. Therefore, it is necessary to establish numerical simulations of the observed weld pool phenomena.

When considering the observed increase in penetration depth by remelting the mill scale of steel plates, the question of possible applications of such an approach arises. Steels of the considered upper strength level are mostly processed by gas metal arc welding or submerged arc welding. In contrast to these welding processes, the fluid flow of the weld pool in GTA welding is influenced much stronger by the chemical composition. The expected effect in GMA welding would be lower due to the differing impact of the consumable electrode on the fluid flow. If steel manufacturers are able to deliver steel grades with intentionally set uniform scale layer thickness, the use of arc welding processes with increased productivity at reduced heat input levels could be realized in the future. A more sophisticated approach is already known by surfacing the steel plates with activating flux agents [14].

5 Conclusions

From the presented work, the following conclusions can be drawn:

1. TIG remelting of a mill scale on the surface of high-strength steel heavy plates leads to longer cooling times.
2. Depending on the chemical composition of the base metal, constant arc energy leads to different cooling times.
3. A strong influence on the weld bead geometry in most investigated materials is visible. A welded mill scale leads to increased penetration depth and smaller weld bead width for high weld metal oxygen contents and low sulfur contents.

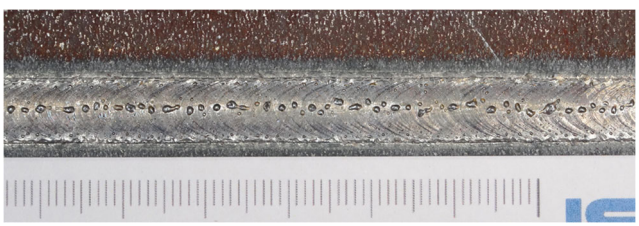

Fig. 11 Weld bead appearance of S960M mill scale-covered sample

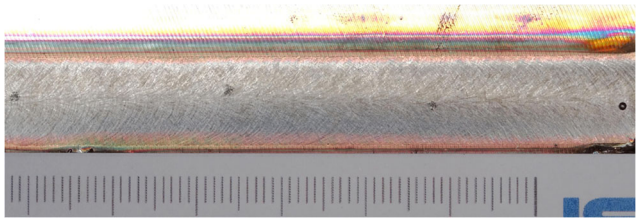

Fig. 12 Weld bead appearance of S960M scale-free surface sample

4. The most striking difference between ground samples and scale-covered samples concerning their chemical composition is the higher oxygen content of the weld metal.
5. For the steels under investigation, the visibility of the effect is supposed to be caused by their low sulfur content

6 Summary

In this work, five high-strength steel grades were compared with respect to the resulting weld bead geometry when GTA remelting was applied. The GTA remelting of mill scale on the surface of steel plates leads to changed weld pool behavior, resulting in deeper penetration and narrower welds. Since the chemical composition of the weld metal changed only marginally, when the scale layer was left on the surface, it can be assumed that the change in cooling times is mostly related to the varying heat dissipation mode. As a result, only the different oxygen content in the weld pool led to deep penetration. The average mill scale thickness is therefore the most important parameter for influencing the weld bead geometry when the scale layer is left on the surface of low sulfur high-strength steels. No substantial deterioration of hardness values could be observed. Nevertheless, it is suggested that the influence of higher oxygen content on ductility and toughness should be examined.

Acknowledgments Open Access funding provided by Projekt DEAL. All presented investigations were conducted in the context of the Collaborative Research Centre SFB1120 “Precision Melt Engineering” at RWTH Aachen University. For sponsorship and support, we wish to express our sincere gratitude.

Funding information This study was funded by the German Research Foundation (DFG), Project ID 236616214.

References

1. Grill R, Egger R, Mayrhofer F (2010) Herstellung und Verarbeitung moderner hochfester Grobbleche. BHM Berg- und Hüttenmännische Monatshefte 155-5:207–212. https://doi.org/10.1007/s00501-010-0564-9
2. Schaupp T, Schroepfer D, Kromm A, Kannengiesser T (2014) Welding residual stress distribution of quenched and tempered and thermo-mechanically hot rolled high strength steels. Adv Mater Res 996:457–462. https://doi.org/10.4028/www.scientific.net/AMR.996.457
3. Xianglong Y, Zhengyi J, Jingwei Z, Dongbin W, Cunlong Z, Qingxue H (2015) Crystallographic texture based analysis of Fe3O4/α-Fe2O3 scale formed on a hot-rolled microalloyed steel, ISIJ international. Vol. 55(1):278–284. https://doi.org/10.2355/isijinternational.55.278
4. Sun, Weihua, A study on the characteristics of oxide scale in hot rolling of steel, PhD thesis, School of Mechanical, Materials and Mechatronic Engineering, University of Wollongong, 2005
5. DIN EN ISO 1011-2: Welding – Recommendations for welding of metallic materials – Part 2: Arc welding of ferritic steels
6. Chen RY and Yuen WYD, Oxide-scale structures formed on commercial hot-rolled steel strip and their formation mechanisms, Oxid Met, 56, Nos. 1/2, 2001 https://doi.org/10.1023/A:1010395419981
7. Heiple CR, Roper JR, Stagner RT, Aden RJ (1983) Surface active element effects on the shape of GTA, laser, electron beam welds. Weld J:72s–77s
8. Heiple CR, Roper JR (1982) Mechanism for minor element effect on GTA fusion zone geometry. Weld J:97s–102s
9. Sharma R, Reisgen U (2018) Assessment of mechanical properties in high-strength steel weld metals by means of phase transformation temperature. Weld World 62:1227. https://doi.org/10.1007/s40194-018-0605-7
10. N.N, TK Steel, Recommendations for welding of XABO 1100, 2004
11. Sharma R, Reisgen U (2016) 'Cooling curve based estimation of mechanical properties in high strength steel welds', Proceedings of Thermec 2016, Graz. Mat Sci Forum 879:1760–1765 https://doi.org/10.4028/www.scientific.net/MSF.879.1760
12. Influence of oxygen content on microstructure and inclusion characteristics of bainitic weld metals, Jun Seok Seo, Changhee Lee, Hee Jin Kim, 2013 53 ISIJ, 2 279–285 https://doi.org/10.2355/isijinternational.53.279
13. Grong Ø (1997) Metallurgical modelling of welding, Institute of Materials (London, England), 2nd. Ed.
14. Yushchenko KA, Kovalenko DV, Kovalenko IV (2001) Application of activators for TIG welding of steels and allows. Paton Weld J 07:37–43
15. Schaupp T, Schroepfer D, Kromm A, Kannengiesser T (2017) Welding residual stresses in 960MPa grade QT and TMCP high-strength steels. J Manuf Process 27:226–232. https://doi.org/10.1016/j.jmapro.2017.05.006